OVERSHOOT OPTIMIZED NEWMARK-TYPE METHODS

Elisabeth Köbis* and Markus A. Köbis**†
*Martin Luther University Halle–Wittenberg, Germany.
**Freie Universität Berlin, Germany.

ABSTRACT
We propose a parameter set for the generalized-α class of time integration methods that allows to keep the beneficial damping properties of the algorithm including controllable dissipation of high frequency oscillations as well as second order of convergence for a large problem class. The benefits of the new parameter set are that the introduction of an additional parameter allows to lessen the overshoot behavior in the transient phase leading to a more robust time integration. To assess the performance of the new parameters, we give a numerically tractable definition of overshoot for the class of algorithms and analyze the methods in terms of a multicriteria optimization problem taking overshoot as well as beneficial damping into account. Using nonlinear scalarization techniques, we can then obtain full insight in how well the methods can perform and evaluate the classical as well as the new parameter sets. Some numerical test examples illustrate the findings.

KEYWORDS: Generalized-α method: overshoot phenomenon, differential-algebraic equations; multiobjective optimization; nonlinear scalarization.

MSC: 65P40, 65L80, 90C29, 90C90.

RESUMEN
En este trabajo se propone un conjunto de parámetros para los métodos de integración de tiempo generalizados de clase-α, el cual permite mantener las propiedades de amortiguamiento del algoritmo, incluyendo la disipación controlable de oscilaciones de alta frecuencia, así como el segundo orden de convergencia para una clase grande de problemas. El nuevo conjunto de parámetros introduce un parámetro adicional que permite disminuir el comportamiento de sobrepaso en la fase transitoria, llevando a una integración de tiempo más robusta. Para evaluar el rendimiento de los nuevos parámetros, se presenta una definición numérica del sobre-salto para esta clase. Además se analizan los métodos como un problema de optimización multicriterio teniendo en cuenta el sobresalto y el amortiguamiento beneficioso como criterios. Usando técnicas de escalarización no lineal, se obtiene una visión completa de cómo se comportan los métodos y cómo evaluan el nuevo conjunto de parámetros y el clásico. Algunos ejemplos numéricos ilustran los hallazgos.

PALABRAS CLAVE: Ecuaciones diferenciales algebraicas, escalarización no lineal, Método α generalizado, optimización multiobjetivo, sobresalto.

1. INTRODUCTION

The generalized-α method [6] has been proposed as a second order extension of the classical time integration methods of Newmark [25]. It offers the possibility to use a single parameter $\varrho_\infty \in [0, 1]$ to control the stability behavior of the method and therefore compromise between small error constants and structure preservation [15] in case of $\varrho_\infty \approx 1$ on the one hand and increased robustness of the method by means of fast annihilation of high-frequency-low-amplitude artifacts in the model for $\varrho_\infty \approx 0$.

†markus.koebis@fu-berlin.de.

Nevertheless, it is known [5, 17] that these two goals are not the only objectives to aim at when designing integration algorithms for technical simulations or structural dynamics. The *overshoot phenomenon* describes spurious oscillations in the transient phase of the time integration which are usually quickly damped out but may cause inaccurate computational results, especially for complex computations involving projection methods [3], strongly varying step sizes or interfaces to other components in a complex model.
The prominent parameter set of Chung and Hulbert [6] is constructed in a way to minimize the low-frequency dissipation behavior of the algorithm without consideration of overshoot. It has recently been shown [2] that the large tendency for overshoot using this parameter set can be explained by the degenerate Jordan canonical form of the one-step amplification matrix [21] of the method. In this work, we suggest a new parameter set which allows to keep the comfortable structure of the algorithm while—through the introduction of an additional parameter—it also allows for a smooth transition to methods with lucidly less over-reaction and spurious oscillations.
To value this new parameter set and gain a thorough understanding, we propose a simple mathematical framework in which we treat the optimization process of the algorithms parameters as a multi-objective optimization problem with the 'tendency of overshoot' and the 'optimal overall dissipation behavior' as objectives. Once this framework is established, we can use nonlinear scalarization methods [13] to further improve the parameters and underline the performance for some well-studied benchmark problems from the literature.
We emphasize that it is very easy to adapt existing codes to the new proposed algorithms since we only change parameters and not the algorithm itself and that due to the nonconvex nature of the optimization problem, nonlinear techniques are indispensable for the acquired results.
The rest of this paper is organized as follows: In Section 2. we state the problem class of the dynamic (mechanical) systems under consideration, give a short outline on known theoretical results and methods for the analysis of Newmark methods and shortly review the most important stability results from the literature. In Section 3. we introduce the novel parameter set *Gen(ϱ_∞, ϕ_0)* and explain its construction before we develop and utilize a general framework that allows for a mathematical substantiation of the overshoot phenomenon and its optimization in Section 4. Section 5. contains some numerical experiments demonstrating the benefits of the optimization before the work is summarized in Section 6, where we also provide some aspects of further investigations.

2. STABILITY AND OVERSHOOT

We consider second order differential-algebraic initial value problems of the form [16]

$$\begin{aligned} \mathbf{M}(\boldsymbol{q}(t))\ddot{\boldsymbol{q}}(t) &= \boldsymbol{F}(\boldsymbol{q}(t), \dot{\boldsymbol{q}}(t), \boldsymbol{\lambda}(t)), \\ \mathbf{0} &= \boldsymbol{\Phi}(\boldsymbol{q}(t), \dot{\boldsymbol{q}}(t), \boldsymbol{\lambda}(t)), \quad \boldsymbol{q}(t_0) = \boldsymbol{q}_0,\ \dot{\boldsymbol{q}}(t_0) = \dot{\boldsymbol{q}}_0,\ (t \in [t_0, t_{\text{end}}]) \end{aligned} \tag{2.1}$$

with a regular (mass) matrix $\mathbf{M}\colon \mathbb{R}^{n_{\boldsymbol{q}}} \to \mathbb{R}^{n_{\boldsymbol{q}} \times n_{\boldsymbol{q}}}$, the vector of generalized forces $\boldsymbol{F}\colon \mathbb{R}^{2n_{\boldsymbol{q}}+n_{\boldsymbol{\lambda}}} \to \mathbb{R}^{n_{\boldsymbol{q}}}$ and the *constraint function* $\boldsymbol{\Phi}\colon \mathbb{R}^{2n_{\boldsymbol{q}}+n_{\boldsymbol{\lambda}}} \to \mathbb{R}^{n_{\boldsymbol{\lambda}}}$ which are all assumed sufficiently smooth but may involve arbitrarily nonlinear components. In the ODE-case, $n_{\boldsymbol{\lambda}}$ might be zero. From a physical perspective, the state vector $\boldsymbol{q}(t) \in \mathbb{R}^{n_{\boldsymbol{q}}}$ describes positions and rotational degrees of freedom, while $\dot{\boldsymbol{q}}(t)$ and $\ddot{\boldsymbol{q}}(t)$ are the respective (angular) velocities and accelerations and $\dot{(\cdot)} := \mathrm{d}(\cdot)/\mathrm{d}t$ denotes differentiation with respect to the time variable t. The Lagrange multipliers $\boldsymbol{\lambda}(t) \in \mathbb{R}^{n_{\boldsymbol{\lambda}}}$ constitute physically artificial values ensuring the constraint fulfillment $\boldsymbol{\Phi} = \mathbf{0}$ for all $t \in [t_0, t_{\text{end}}]$. In this general setting we can cope with purely differential equations without constraints as well as the index-3, 2 and 1 formulations of multibody system dynamics, see [10], even in the case of nonholonomic constraints or friction forces in one unified framework. The obtained new methods are therefore applicable in a wide range of practical problems from various areas of mechanics.
The class of time integration methods we address here is defined by four parameters α_f, α_m, β, and

γ. For the problem (2.1) and time integration step size $h_n > 0$, one time step reads [1, 6]

$$\boldsymbol{q}_{n+1} = \boldsymbol{q}_n + h_n \boldsymbol{v}_n + h_n^2(\tfrac{1}{2} - \beta)\boldsymbol{a}_n + h_n^2 \beta \boldsymbol{a}_{n+1}\,, \tag{2.2a}$$

$$\boldsymbol{v}_{n+1} = \boldsymbol{v}_n + h_n(1-\gamma)\boldsymbol{a}_n + h_n \gamma \boldsymbol{a}_{n+1}\,, \tag{2.2b}$$

$$(1-\alpha_m)\boldsymbol{a}_{n+1} + \alpha_m \boldsymbol{a}_n = (1-\alpha_f)\dot{\boldsymbol{v}}_{n+1} + \alpha_f \dot{\boldsymbol{v}}_n\,, \tag{2.2c}$$

$$\mathbf{M}(\boldsymbol{q}_{n+1})\dot{\boldsymbol{v}}_{n+1} = \boldsymbol{F}(\boldsymbol{q}_{n+1}, \boldsymbol{v}_{n+1}, \boldsymbol{\lambda}_{n+1})\,, \tag{2.2d}$$

$$\mathbf{0} = \boldsymbol{\Phi}(\boldsymbol{q}_{n+1}, \boldsymbol{v}_{n+1}, \boldsymbol{\lambda}_{n+1})\,. \tag{2.2e}$$

The state variables $\boldsymbol{q}_n$, $n = 0, 1, \ldots$ therefore denote numerical approximations to $\boldsymbol{q}(t_n)$ at the n-th time step $t_{n+1} := t_n + h_n$, $n = 0, 1, \ldots$, while $\boldsymbol{v}_n$ and $\dot{\boldsymbol{v}}_n$ approximate $\dot{\boldsymbol{q}}(t_n)$ and $\ddot{\boldsymbol{q}}(t_n)$. The *acceleration-like variables* $\boldsymbol{a}_n$ are coupled to the actual approximations $\dot{\boldsymbol{v}}_n$ by the weighted-sum relation (2.2c) making the generalized-α algorithm a 'one-step-multivalue method' [21], i. e. a multistep method allowing for a (rather simple) onestep implementation.

Remark 2.1. *We will always assume that*

$$\beta \neq 0\,, \quad \alpha_f \neq 1\,,$$

are fulfilled. This requirement ensures well-definition of error-recursion related terms we are going to establish. These assumptions practically do not restrict the generality of our results as they are necessary for stability of the methods anyway, as will become clear in Proposition 2.1. below.

Using Taylor expansions of the exact solution, plugging in the equilibrium conditions (2.2d) and (2.2e) and comparing powers of the time step size reveals that the method is second order accurate (for position and velocity variables and constant time step size $h_n = h$, $n = 0, 1, \ldots$) provided that

$$\gamma = \frac{1}{2} - \alpha_m + \alpha_f\,, \tag{2.3}$$

is fulfilled, see [6]. Since we are dealing with a multistep scheme in a differential-algebraic framework, the accuracy from the above order condition (2.3) is less important than the stability conditions which, stated rather simplified, ensure that the error recursion for a large number of (possibly very small) time integration steps, the numerical errors do not grow exponentially [8, 16]. All stability notions that we address in this paper are defined in the appendix.

Proposition 2.1. (Classical stability of Newmark-type methods, [11]) *The second order Newmark-type method* (2.2) *is*

1. *zero stable, i. e. computes stable solutions for* $\max_n h_n \to 0$*, provided that*

$$\alpha_m \leq \frac{1}{2} \quad \textit{or} \quad \alpha_m = \alpha_f\,. \tag{2.4}$$

2. *strictly stable at infinity and unconditionally stable if and only if*

$$\alpha_m < \alpha_f < \frac{1}{2}\,, \quad \frac{1}{4} + \frac{1}{2}(\alpha_f - \alpha_m) < \beta\,. \tag{2.5}$$

The second stability notions involve the analysis of the method for the linear test equation of the harmonic oscillator, see [9]. The proofs rely on the onestep error recursion which we investigate further below. In the case $\alpha_m = \alpha_f$, the algorithm degenerates to the classical time integration scheme of Newmark [25] which has already extensively been studied in the literature and is only second order accurate for the trapezoidal rule $\gamma = \frac{1}{2}$, $\beta = \frac{1}{4}$ which incorporates no numerical damping $\varrho_\infty = 1$ and is therefore not additionally taken into account from now on. For this parameter setting, the error recursion can be substantially simplified (to a 2-by-2 structure) and dealt with analytically, see [12].

3. A NEW PARAMETER SET WITH CONTROLLABLE OVERSHOOT BEHAVIOR

The original parameter set of the algorithm (2.2) in the given form are dependent solely on one value which can be provided by the user. Using this *numerical damping parameter* $\varrho_\infty \in [0,1]$, the coefficients read

$$\text{CH}(\varrho_\infty): \quad \alpha_m = \frac{2\varrho_\infty - 1}{\varrho_\infty + 1}\,, \quad \alpha_f = \frac{\varrho_\infty}{\varrho_\infty + 1}\,, \quad \beta = \frac{1}{(1+\varrho_\infty)^2}\,, \quad \gamma = \frac{3-\varrho_\infty}{2+2\varrho_\infty}\,. \tag{3.1}$$

In [6], the authors develop the algorithm as a generalization of the two already established Newmark-type methods of Hilber, Hughes, and Taylor (HHT, [18]) with

$$\text{HHT:} \quad \alpha_m = 0,\ \alpha_f = \frac{1-\varrho_\infty}{\varrho_\infty + 1},\ \beta = \frac{1}{(\varrho_\infty+1)^2},\ \gamma = \frac{3-\varrho_\infty}{2+2\varrho_\infty},\ \varrho_\infty \in [\tfrac{1}{2}, 1]\,, \tag{3.2}$$

and the algorithm of Wood, Bossak, and Zienkiewicz (Bossak-Newmark, WBZ, [32]) where the parameters are given by

$$\text{WBZ:} \quad \alpha_m = \frac{\varrho_\infty - 1}{\varrho_\infty + 1},\ \alpha_f = 0,\ \beta = \frac{1}{(\varrho_\infty+1)^2},\ \gamma = \frac{3-\varrho_\infty}{2+2\varrho_\infty},\ \varrho_\infty \in [0, 1]\,. \tag{3.3}$$

In any case, the parameter ϱ_∞ serves as the only user input and controls the behavior of the numerical solutions for large frequency problems. Additionally, all these methods inherit the so-called *optimal dissipation relation* from the classical Newmark integration scheme [25], i. e.

$$\beta = \frac{(\gamma + 1/2)^2}{4}\,, \tag{3.4}$$

which is the analytically optimal choice (with respect to numerical damping) for this easier family (with $\alpha_m = \alpha_f$). The requirements for a profitable and robust time integration scheme in the engineering sciences, however, comprise more than this.

Design paradigms for time integration methods in structural dynamics According to [21], an ODE time integration method for structural mechanics should serve the following properties:

(a) It should be (at least) second order accurate.

(b) It should show unconditional linear stability.

(c) Each time integration step should necessitate the solution of no more than one set of implicit equations of dimension $n_{\boldsymbol{q}} + n_{\boldsymbol{\lambda}}$.

(d) It should be self-starting, i. e., except of the initialization of all involved quantities from the initial data, no further computations should be necessary to start the time integration.

(e) The algorithmic damping of high frequency modes should be controllable by the user using a parameter. Advisable are schemes that allow for a smooth transition from no numerical damping $\varrho_\infty = 1$ to instantaneous annihilation $\varrho_\infty = 0$ (L-stability).

For requirements (a) and (b), the famous results of Dahlquist [9] lay the foundation: The so-called *second Dahlquist barrier* [16] states, that a linear multistep scheme (the generalized-α method (2.2) can equivalently be stated as a partitioned linear multistep method, see [23, Remark 4.2] and [7]) that is unconditionally linear stable can have at most order two of consistency. The "best" among those methods is the trapezoidal rule (Verlet scheme) judging only from the viewpoints of a minimal error constant [9] and structure preservation [15]. For the development of the new parameter choice "Gen(ϱ_∞, ϕ_0)" below, we will thus add the condition that

(e$_2$) It should be possible to obtain the trapezoidal rule when the numerical damping is switched off, i.e. when $\varrho_\infty \to 1$.

Condition (c) is naturally fulfilled for all methods in the family (2.2) which is probably one of the main reasons for their steady success in the areas of mechanical system engineering and structural dynamics. One can, nevertheless, observe that HHT falls short of requirement (e): An L-stable version is not achievable but instead the possible values of the numerical dissipation only range from $\varrho_\infty = \frac{1}{2}$ to $\varrho_\infty = 1$, where the method coincides with the trapezoidal rule.
Overshoot comes in at requirement (d) since an out-of-the-box initialization should encompass a stable and free-of-artifacts transient phase. For an introduction to the construction principles of the methods below we will shortly review the basics of the linear analysis of Newmark-type methods and the theoretical foundations of overshoot. All details can be found in [4, 17, 21].
The initial point for the numerical analysis of the methods is the scalar second order differential equation of the damped harmonic oscillator

$$\ddot{q}(t) + 2\xi\omega\dot{q}(t) + \omega^2 q(t) = 0\,, \quad q(0) = q_0\,,\ \dot{q}(0) = \dot{q}_0\,, \quad (\omega,\, \xi \in \mathbb{R})\,, \tag{3.5}$$

which for weak damping $0 \le \xi < 1$ obeys the analytic solution

$$q(t) = \mathrm{e}^{-\xi\omega t}\left(C_1\cos(\bar{\omega}t) + C_2\sin(\bar{\omega}t)\right)\,, \quad C_1 = q_0\,,\ C_2 = (q_0\xi\omega + \dot{q}_0)/\bar{\omega}\,, \quad \bar{\omega} = \omega\sqrt{1-\xi^2}\,. \tag{3.6}$$

From a stability point of view, the most important observation is the global boundedness of solutions (3.6) for any values of the frequency parameter ω. One step (with constant time step size $h_n = h$, $n = 0, 1, \ldots$) can thus be stated as a linear update formula.

$$\begin{pmatrix} 1 & 0 & -\beta \\ 0 & 1 & -\gamma \\ (1-\alpha_f)z^2 & (1-\alpha_f)w & 1-\alpha_m \end{pmatrix} \begin{pmatrix} q_{n+1} \\ hv_{n+1} \\ h^2a_{n+1} \end{pmatrix} = \begin{pmatrix} 1 & 1 & 1/2-\beta \\ 0 & 1 & 1-\gamma \\ -\alpha_f z^2 & -\alpha_f w & -\alpha_m \end{pmatrix} \begin{pmatrix} q_n \\ hv_n \\ h^2a_n \end{pmatrix}\,, \tag{3.7}$$

with $z := h\omega$, $w := z\xi$. As, locally, all smooth dynamical systems in technical system simulation can be approximated by linear surrogate models and (apart from external forces) the discretized finite-element models from structural dynamics are in this linear form, it serves—despite its rather simple structure and low dimensionality—as a viable model equation for studying the behavior of the methods. This approach can also be seen as a quasi-standard, cf. [12, 21].
Since no external forces are active in (3.5) (no inhomogeneity terms in the right hand side), the numerical solution of the time integration scheme at any point $t_n = n \cdot h$ is explicitly given by $(q_n, hv_n, h^2a_n)^\top = (\mathbf{T}(z))^n(q_0, hv_0, h^2a_0)$ with given initial values q_0, v_0, and an approximation $a_0 \approx \ddot{q}(0)$. The involved *error amplification matrix* $\mathbf{T}(z)$ for the most important case of physically undamped systems ($\xi = 0$) is, after plugging in the second order condition (2.3), explicitly given by

$$\mathbf{T}(z) = \begin{pmatrix} \frac{\alpha_f\beta z^2+\alpha_m-1}{(\alpha_f-1)\beta z^2+\alpha_m-1} & \frac{\alpha_m-1}{(\alpha_f-1)\beta z^2+\alpha_m-1} & \frac{\alpha_m+2\beta-1}{2((\alpha_f-1)\beta z^2+\alpha_m-1)} \\ \frac{(2\alpha_f-2\alpha_m+1)z^2}{2((\alpha_f-1)\beta z^2+\alpha_m-1)} & 1-\frac{(\alpha_f-1)(2\alpha_f-2\alpha_m+1)z^2}{2((\alpha_f-1)\beta z^2+\alpha_m-1)} & \frac{-2\alpha_f^2z^2+(-2\alpha_m-4\beta+1)z^2+\alpha_f\left((2\alpha_m+4\beta+1)z^2+4\right)-2}{4((\alpha_f-1)\beta z^2+\alpha_m-1)} \\ \frac{z^2}{(\alpha_f-1)\beta z^2+\alpha_m-1} & -\frac{(\alpha_f-1)z^2}{(\alpha_f-1)\beta z^2+\alpha_m-1} & \frac{(\alpha_f-1)(2\beta-1)z^2+2\alpha_m}{2((\alpha_f-1)\beta z^2+\alpha_m-1)} \end{pmatrix}\,. \tag{3.8}$$

The limit of infinite stiffness ("infinite frequency" oscillations) can also be evaluated analytically:

$$\mathbf{T}(\infty) = \lim_{z\to\infty}\mathbf{T}(z) = \begin{pmatrix} \frac{\alpha_f}{\alpha_f-1} & 0 & 0 \\ -\frac{2\alpha_f-2\alpha_m+1}{2\beta-2\alpha_f\beta} & \frac{-2\alpha_f+2\alpha_m+2\beta-1}{2\beta} & \frac{-2\alpha_f+2\alpha_m+4\beta-1}{4\beta} \\ \frac{1}{(\alpha_f-1)\beta} & -\frac{1}{\beta} & 1-\frac{1}{2\beta} \end{pmatrix}\,. \tag{3.9}$$

From this, it is evident that the stability behavior of the numerical solutions depends on the growth of matrix powers $\mathbf{T}^n$. For the long-term behavior, it is convenient to simply take the spectral radius

$\sigma(\mathbf{T})$ (maximum absolute value of eigenvalues of $\mathbf{T}$) as a measure for this growth. For an analysis of the short-term behavior, however, one should take into account that the error amplification matrix is non-normal [31] and a more detailed look is necessary: As has been pointed out by various authors [2, 5, 17], overshoot can be studied by using the Jordan canonical form

$$\mathbf{T}(\infty) =: \mathbf{C}\mathbf{J}_*\mathbf{C}^{-1}\,, \tag{3.10}$$

which for the most prominent representants, CH(ϱ_∞), HHT, and WBZ (see (3.1), (3.2), (3.3) above) are given by

$$\begin{aligned}
\mathbf{J}_{\mathrm{CH}} &= \begin{pmatrix} -\varrho_\infty & 1 & 0 \\ 0 & -\varrho_\infty & 1 \\ 0 & 0 & -\varrho_\infty \end{pmatrix}, \\
\mathbf{J}_{\mathrm{HHT}} &= \begin{pmatrix} -\varrho_\infty & 1 & 0 \\ 0 & -\varrho_\infty & 0 \\ 0 & 0 & (\varrho_\infty-1)/(2\varrho_\infty) \end{pmatrix}, \ \left(\varrho_\infty > \frac{1}{2}\right), \quad \mathbf{J}_{\mathrm{HHT}} = \begin{pmatrix} -\varrho_\infty & 1 & 0 \\ 0 & -\varrho_\infty & 1 \\ 0 & 0 & -\varrho_\infty \end{pmatrix}, \ \left(\varrho_\infty = \frac{1}{2}\right), \\
\mathbf{J}_{\mathrm{WBZ}} &= \begin{pmatrix} -\varrho_\infty & 1 & 0 \\ 0 & -\varrho_\infty & 0 \\ 0 & 0 & 0 \end{pmatrix},
\end{aligned} \tag{3.11}$$

such that for the matrix powers $(\mathbf{T}(\infty))^n$ the non-diagonal entries cause an amplification since the values $(\mathbf{J}^n_{\mathrm{CH}})_{1,3} = \frac{1}{2}n(n-1)(-\varrho_\infty)^{n-2}$, $(\mathbf{J}^n_{\mathrm{HHT/WBZ}})_{1,2} = n(-\varrho_\infty)^{n-1}$ may grow large unless the damping parameter is chosen very small, cf. Figure 3 below.

The design idea behind our new proposal for the parameter choice is to keep the requirement that the absolute values of the eigenvalues of $\mathbf{T}(z)$ in the limit case $z \to \infty$ attain the value of ϱ_∞ but make sure that, whenever a method with numerical damping is required, the eigenvalues remain separate of each other. This way, it is assured that the Jordan canonical form is a diagonal matrix and no off-diagonal elements can cause error growth. Since $\mathbf{T}(\infty)$ is a real valued 3x3-matrix, at least one eigenvalue $\lambda_1(\mathbf{T}(\infty))$ is also-real valued (the "spurious root" [21]). For a good low-frequency approximation, it is advisable to find parameters such that the two other eigenvalues (the "principal roots"; their branches for varying z are locally well-defined since for $z = 0$, the amplification matrix has a double eigenvalue $\lambda_2(\mathbf{T}(0)) = \lambda_3(\mathbf{T}(0)) = 1$ and a spurious root at $\lambda_1(\mathbf{T}(0)) = 0$) are not real-valued in a neighborhood of $z = 0$.

As opposed to the parameter sets from the literature in which these roots attain a real value for $z \to \infty$, we will furthermore require that they lie on the complex unit circle of radius ϱ_∞. With respect to the design paradigm (e_2) stated above, we add another parameter $\phi_0 \in (0, \pi)$ and the requirement

$$\arg(\lim_{z\to\infty} \lambda_2(\mathbf{T}(z))) \stackrel{!}{=} \pi - (\pi - \phi_0)(1 - \varrho_\infty)\,, \quad \varrho_\infty \in (0, 1]\,.$$

Keeping $\alpha_f = \varrho_\infty/(\varrho_\infty + 1)$, such that the spurious root tends towards $-\varrho_\infty$ for $z \to \infty$, we have enough equality constraints to attain a nonlinear system for the parameters which can uniquely be solved for the parameters of the method (2.2) as functions of ϱ_∞ and ϕ_0.

This leads to the **parameter set**

$$\left.\begin{aligned}
\alpha_m &= \frac{\varrho_\infty}{\varrho_\infty+1} + \frac{\varrho_\infty^2 - 1}{1 + \varrho_\infty^2 - 2\varrho_\infty\cos(\phi_0 - \phi_0\varrho_\infty + \pi\varrho_\infty)}\,, \\
\alpha_f &= \frac{\varrho_\infty}{\varrho_\infty+1}\,, \\
\beta &= \frac{1}{1 + \varrho_\infty^2 - 2\varrho_\infty\cos(\phi_0 - \phi_0\varrho_\infty + \pi\varrho_\infty)}\,, \\
\gamma &= \frac{1}{2} - \alpha_m + \alpha_f\,.
\end{aligned}\right\} \mathrm{Gen}(\varrho_\infty, \phi_0) \tag{3.12}$$

Note that for $\phi_0 \to \pi$, the methods approach the CH(ϱ_∞) setting. The numerical dissipation and dispersion behavior of these methods is slightly inferior compared to CH(ϱ_∞) as we will see in Figure 2 below, but the overshoot in the sense of the above growth of Jordan block powers is diminished. With respect to the requirements stated above, our method naturally fulfills (a), (c), (d), (e), and (e_2) since it builds up upon the known Newmark-type methods with other parameters and the parameters were chosen using the conditions (e) and (e_2). It remains to be shown that theses methods are also zero- and unconditionally stable as this was not declared part of the method's construction. Proposition 2.1. explicitly gives necessary and sufficient conditions for stability. Instead of giving a formal proof via algebraic manipulations, we show that all conditions of Proposition 2.1. are fulfilled graphically in Figure 1. All the shown surface plots remain clearly non-negative which strongly indicates that the

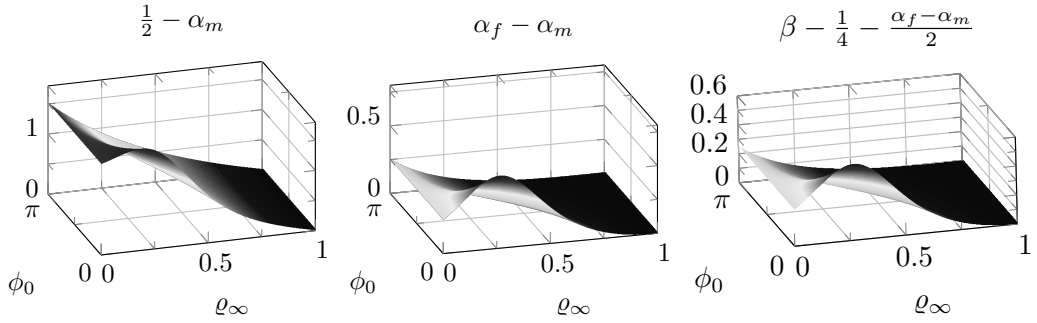

Figure 1: Numerical verification of the stability requirement for the parameter set Gen(ϱ_∞, ϕ_0)

parameters that depend smoothly on the two parameters ϱ_∞ and ϕ_0 form stable methods.

Remark 3.2. *As for the stability requirements, it is also crucial for practically viable methods to guarantee* bounded parameters *which is important for an internally stable computation and bounded error constants for the third order terms as well. For the Gen(ϱ_∞,ϕ_0) parameter set, it can be shown that*

$$\alpha_f \in [0, \tfrac{1}{2}), \qquad \alpha_m \in [-1.1761, \tfrac{1}{2}), \qquad \beta \in (\tfrac{1}{4}, 1.41326], \qquad \gamma \in (\tfrac{1}{2}, 1.8423],$$

are fulfilled for all $\varrho_\infty \in [0, 1)$ and all $\phi_0 \in (0, \pi)$. For the Chung/Hulbert parameter set (3.1) *it holds*

$$\alpha_f \in [0, \tfrac{1}{2}), \qquad \alpha_m \in [-1, \tfrac{1}{2}), \qquad \beta \in (\tfrac{1}{4}, 1], \qquad \gamma \in (\tfrac{1}{2}, \tfrac{3}{2}],$$

for all $\varrho_\infty \in [0, 1)$.

In Figure 2 we display the spectral radius of the amplification matrix $\mathbf{T}(z)$ as a function of the product of time step size and frequency of the system $z = h\omega$ in a semi-logarithmic scale, compare e. g. [17]. As required, for large values of z, the absolute value of the eigenvalues approaches the given numerical damping ϱ_∞. For comparison, we included the corresponding curves for the backward differentiation formulae (BDF, cf. [16]) and the parameter set of Chung/Hulbert which could have also been attained by formally setting $\phi_0 = \pi$. One can observe that the low-frequency behavior of Gen(ϱ_∞, ϕ_0) is slightly influenced.
The algorithms show stronger damping for medium frequency which might be regarded as inferior to CH(ϱ_∞) as the methods might also damp out components of the solution that are in a mechanically relevant frequency range, see Definition 4.2. below. On the other hand, one could argue that the steeper descent in case of the the Gen(ϱ_∞,ϕ_0) parameters is advantageous since it does not smear the frequency response of the method so strongly an thereby produces more reliable results.

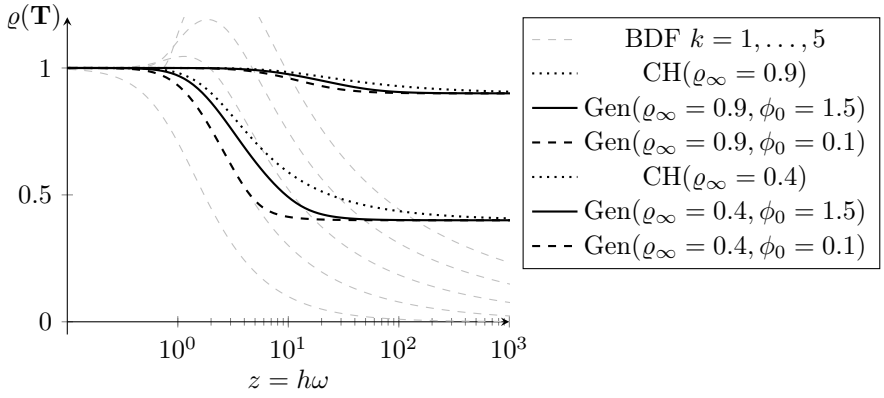

Figure 2: Spectral radii of amplification matrices for CH(ϱ_∞) and Gen(ϱ_∞, ϕ_0) for varying z

Remark 3.3. *Note that the optimal dissipation relation* (3.4) *is not fulfilled for this set of parameters. From the viewpoint of the above analytic consideration, it ensures that the principal roots attain a real value for $z \to \infty$. The design idea of Gen(ϱ_∞, ϕ_0) was exactly to avoid this behavior.*

Bounding the growth of the Jordan matrices in (3.10) is not indispensably enough to also avoid overshoot; the transient error growth is guided by powers of the amplification matrix $\mathbf{T}$ itself. In Figure 3 we show the growth of the norm of the matrix powers $\mathbf{J}^n$ and $(\mathbf{T}(\infty))^n$ over n (representing the number of time integration steps) for the well-known parameter sets (3.1) and (3.2) as well as two representatives. We will use the same values in the definition of the measure of overshoot in Section 4. below. Note that, formally, we ruled out the case $\phi_0 = 0$ in the definition of the methods but since this defines the limit case when seen as the 'distance from CH(ϱ_∞)', the plots also present the boundaries of our approach. Note also that in the figures on the left, the plots for Gen($\varrho_\infty, 0$) and Gen($\varrho_\infty, \pi/4$) coincide as the Jordan canonical forms are equivalent.
At first, we observe that, as intended, the norms of matrix powers that directly affect the errors of the integration method in the first time steps are indeed much faster declining for the Gen(ϱ_∞,ϕ_0) parameters than for the two established settings. This is strongly to be seen in the left plots of Figure 3, for the right sides we emphasize that the norm and power function, contrary to the Jordan canonical forms, is a smooth function and the initial growth cannot be immediately ruled out.

Remark 3.4. *One could argue that the choice $\lambda_1^\infty = -\varrho_\infty$ is rather arbitrary and instead also $\lambda_1^\infty = +\varrho_\infty$ could have been chosen. This case also leads to a nonlinear system which can analytically be solved for the parameters as functions of ϱ_∞ and ϕ_0*

$$\begin{aligned}
\alpha_m &= \frac{1 - \varrho_\infty^2 + 2\varrho_\infty^3 - 2\varrho_\infty^2 \cos(\phi_0 - \phi_0\varrho_\infty + \pi\varrho_\infty)}{(\varrho_\infty - 1)(1 + \varrho_\infty^2 - 2\varrho_\infty \cos(\phi_0 - \phi_0\varrho_\infty + \pi\varrho_\infty))}\,, \\
\alpha_f &= \frac{\varrho_\infty}{\varrho_\infty - 1}\,, \\
\beta &= \frac{1}{1 + \varrho_\infty^2 - 2\varrho_\infty \cos(\phi_0 - \phi_0\varrho_\infty + \pi\varrho_\infty)}\,, \\
\gamma &= \frac{1}{2} - \alpha_m + \alpha_f\,.
\end{aligned}$$

This approach, however, on the one hand leads to significantly less performance with regards to the low-frequency behavior (i. e., the numerical damping measure, see Section 4. below), and on the other hand violates requirement (e_2) as we cannot approach the (arguably best) trapezoidal rule. Nevertheless, also

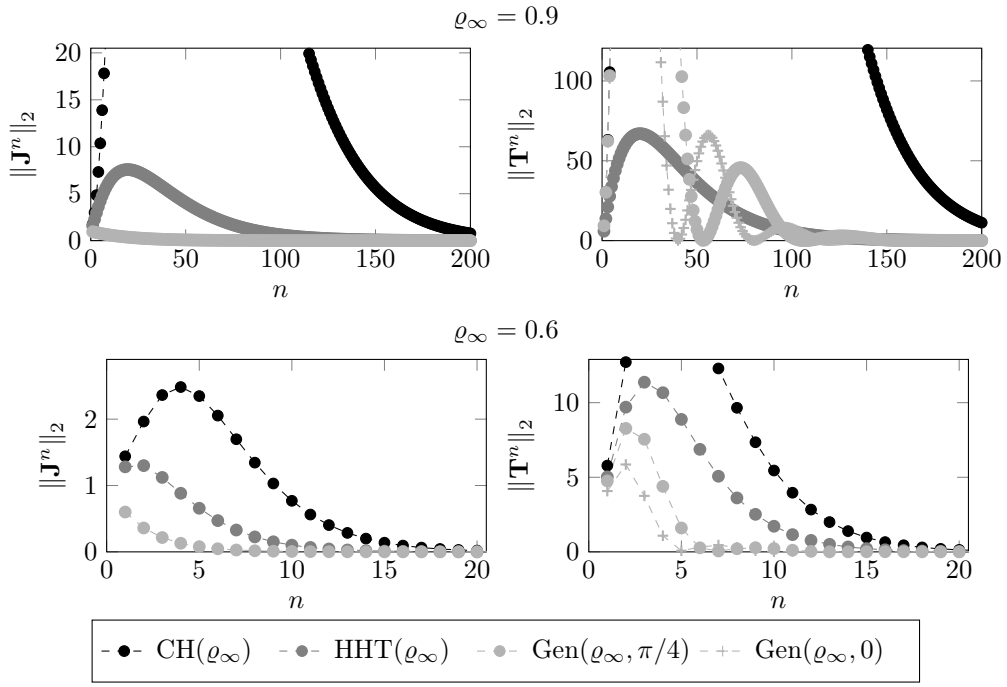

Figure 3: Norm of powers of the Jordan matrices for CH(ϱ_∞), HHT and Gen(ϱ_∞, ϕ_0)

for this parameter set the basic stability properties from Proposition 2.1. are fulfilled for all parameters $\varrho_\infty \in [0, 1)$, $\phi_0 \in (0, \pi)$ *as can be shown by algebraic manipulations as well.*

4. MULTICRITERIA OPTIMIZATION OF THE PARAMETERS

In this section, we will use a vector optimization approach to find out whether it is possible to improve the novel parameters from the previous section. To this end, we will at first give a mathematically tractable definition for our two main design goals.

Definition 4.1. (Measure of overshoot) *For the Newmark-type methods* (2.2)*, let the amplification matrix for* $z \to \infty$ *be denoted by* $\mathbf{T}(\infty)$ *as in* (3.9)*. Furthermore, let a matrix norm* $\|\bullet\|_*$ *be given. The* measure of overshoot $m^*_{\mathrm{os}}(\mathbf{T})$ *is then given by*

$$m^*_{\mathrm{os}}(\mathbf{T}) := \max_{n=0,1,2,\ldots} \|(\mathbf{T}(\infty))^n\|_* \,.$$

From the above short introduction on the numerical analysis of Newmark-type methods, the definition is self-evident: The overshoot phenomenon stems from the transient amplification of spurious error terms in the initial phase of the time integration. If the powers of this amplification matrix grow heavily, this directly results in large overshoot.
Note that the superscript (the asterisk "$(\cdot)^*$" in the definition) is used to indicate the dependency of the actual value of the measure of overshoot from the chosen matrix norm. Because of norm equivalence in $\mathbb{R}^n$, the explicit choice of a norm in the definition does not play an important role for now. As a design objective, we will use the 2-norm, i. e., the maximum singular value of the matrix $\mathbf{T}^n$ which is compatible with the (standard) Euclidean vector-norm and therefore use $m^2_{\mathrm{os}}(\mathbf{T})$ in the experiments below.
The second performance measure is not as straightforward and reads as follows.

Definition 4.2. (Numerical damping measure) *The* numerical damping measure $m_{\mathrm{d}}(\mathbf{T})$ *of a Newmark-type method* (2.2) *with numerical dissipation* $\varrho_\infty = \lim_{z\to\infty}\sigma(\mathbf{T}(z)) \in [0,1)$ *is defined as*

$$m_{\mathrm{d}}(\mathbf{T}) := \frac{\int_{-6}^{6}\left(\sigma(\mathbf{T}(z)) - \varrho_\infty\right) d\lg(z)}{12\cdot(1-\varrho_\infty)}\,, \tag{4.1}$$

where $\lg(\cdot)$ *denotes the logarithm for base* 10 *and* $\sigma(\cdot)$ *signifies the spectral radius.*

From a practical viewpoint, a small numerical damping measure corresponds to a tendency of the method to 'over-damp' the frequency response of the (e. g., mechanical) system which could lead to a violation of the energy balance and remove physically relevant modes in the numerical solution. The scaling in the definition of $m_{\mathrm{d}}(\mathbf{T})$ above is for comparability: A (hypothetical) method showing no numerical dissipation over the entire frequency range $z \in [10^{-6}, 10^{6}]$ thus has a numerical damping measure of one.

Remark 4.5. *The choice of the lower and upper integration limits in* (4.1) *might be regarded as rather arbitrary and could be adapted as could the specific choice of the basis of the logarithm. The important requirement is solely that the relevant frequency range of mechanical systems can be covered. Using* 12 *orders of magnitude is arguably sufficient to cover most mechanical applications.*

Since, at this point, we have no prior knowledge regarding the actual form of the set of feasible points in the parameter space or the objective functions we will approach the vector optimization problem using a very general computational approach that does not rely on any convexity or smoothness assumptions. A very natural way for scalarization that is able to fully cope with any partially ordered space is the Tammer-Weidner (Gerstewitz) nonlinear scalarization.

Definition 4.3. (Nonlinear scalarizing functional [13]) *Let* Y *be a linear topological space,* $C \subseteq Y$ *be a proper closed convex cone, and* $k \in C \setminus \{\mathbf{0}^*\}$ *with* $\mathbf{0}^*$ *denoting the zero-element in* Y*. We introduce the* nonlinear scalarization functional $z^{C,k}(y)\colon Y \to \mathbb{R}\cup\{\pm\infty\}$ *by*

$$z^{C,k}(y) := \inf\{t \in \mathbb{R} \mid y \in tk - C\} \quad \textit{with} \quad \inf\emptyset := +\infty\,.$$

The functional $z^{C,k}(y)$ has been used in various applications to obtain optimality conditions in very general settings. For additional details and a more comprehensive investigation of its properties, we refer to [14]. A way for the efficient numerical calculation of the nonlinear scalarization functional in case of polyhedral ordering cones has been proposed in [30]: If the cone $C \subset Y = \mathbb{R}^n$ can be expressed as

$$C := \{y \in \mathbb{R}^n \mid \mathbf{W}y \in \mathbb{R}^m_{\geq 0}\}\,, \tag{4.2}$$

for some given matrix $\mathbf{W} \in \mathbb{R}^{m\times n}$ where $\mathbb{R}^m_{\geq 0}$ denotes the natural ordering cone and where each row of $\mathbf{W}$ does not only consist of zeros. If, furthermore, it holds $k \in \operatorname{int} C$, then the functional $z^{C,k}$ can be evaluated as

$$z^{C,k}(y) = \max_{l=1,\ldots,m} \frac{\langle \mathbf{W}_{l,:}, y\rangle}{\langle \mathbf{W}_{l,:}, k\rangle}\,,$$

where $\bullet_{l,:}$ denotes the l-th row in matrix $\bullet$. For the special case of the natural ordering cone in $\mathbb{R}^n$, $C = \mathbb{R}^n_{\geq 0}$, it holds $\mathbf{W} = \mathbf{I}_n$ (identity matrix) and therefore

$$z^{C,k}(y) = \max_{i=1,\ldots,n} \frac{y_i}{k_i}\,.$$

At first, it is our goal to treat the task as an unconstrained optimization problem and, after appropriate scalarization, apply the simplex-method of Nelder & Mead [24] as this is known for its robustness in various application contexts. In order to apply this algorithm, we will use penalty techniques for

the constraints in the model to get good approximative solutions. The explicit choice of the penalty function $\phi_{\text{penalty}}(\alpha_m, \alpha_f, \beta, \gamma)$ will be given below.
Using the obtained solutions as initial guesses, we then conduct further optimization runs using an active-set approach, see [26], keeping the constraints exactly fulfilled. Nevertheless, this might still lead to approximations that are not Pareto-optimal since the algorithms only find local minimizers of the objective function

$$f_{\text{obj}}(\alpha_f, \alpha_m, \beta, \gamma; k, \theta) := z^{C,k}(\,(m_{\text{os}}^2(\mathbf{T}), -m_{\text{d}}(\mathbf{T}))^\top\,)\Big|_{\mathbf{T}=\mathbf{T}(z;\alpha_f,\alpha_m,\beta,\gamma)} + \theta \cdot \phi_{\text{penalty}}(\alpha_f, \alpha_m, \beta, \gamma)\,, \quad (\theta \in \{0,1\})\,. \quad (4.3)$$

So, as a post-processing step, we sorted out the falsely identified candidates using the Graef-Younes method [33], see also [22], and then projected these solutions to fulfill all constraints to machine precision. The overall procedure is summarized in the following pseudo-code:

Algorithm for determining efficient parameters

Input: $\varrho_\infty \in [0,1)$, set of vectors $\{k_i \in C\}_{i=1,\dots,n_k}$, polyhedral ordering cone C.
Step 0) Set $S := \emptyset$.
For $i = 1, \dots, n_k$:
  Step 1) Set $\theta := 1$ and $k := k_i$ in the objective function (4.3).
  Step 2) Determine a crude approximation of the objective values by sampling the argument space for $(\alpha_f, \alpha_m, \beta) \in \big([-10, \frac{1}{2}] \times [-10, \frac{1}{2}] \times [\frac{1}{4}, 10]\big)$, $\gamma := \frac{1}{2} - \alpha_m + \alpha_f$.
  Step 3) Use the Nelder-Mead simplex algorithm with
    (a) the best performing values of the sampling in Step 2) in this loop cycle and
    (b) the best performing values in S
  as initial guesses to obtain approximations to new parameter sets.
  Step 4) Set $\theta := 0$ and use an active-set scalar optimization method with
    (a) the best performing values of Step 3) in this loop cycle and
    (b) the best performing values in S
  as initial guesses. Denote the best performing solution by $(\alpha_f^{(i)}, \alpha_m^{(i)}, \beta^{(i)}, \gamma^{(i)})$.
  Set $S := S \cup \{(\alpha_f^{(i)}, \alpha_m^{(i)}, \beta^{(i)}, \gamma^{(i)})\}$.
End For
Step 5) Sample out non-efficient elements of S using the Graef-Younes procedure.
Step 6) Use a higher precision engine and project the parameter sets in S to fulfill all constraints from Proposition 2.1. to machine precision.
Output: New parameter sets S.

The term "best performing" is always to be understood as the parameter sets (not necessarily just one) leading to the lowest objective values for f_{obj} using the current values for θ and k. Note that it is computationally very cheap to calculate the values of the nonlinear scalarization functional $z^{C,k}(y)$ once the vector $y := (m_{\text{os}}^2(\mathbf{T}), -m_{\text{d}}(\mathbf{T}))^\top$ in the objective space has been calculated which is the computationally more demanding part. So, for performance reasons, these values should be stored for the candidates in S as well as the ones obtained in Step 3) of the algorithm.

Remark 4.6. (Technical details) *We emphasize the following specific points regarding the actual calculations:*

- *For all results, we used the natural ordering cone $\mathbb{R}^2_{\geq 0}$ to get all Pareto optimal parameter sets with respect to the given design objectives. We multiplied $m_{\text{d}}^2(\mathbf{T})$ by (-1) for convenience only; the results would have been the same if we had chosen the ordering cone*

$$C := \{(y_1, y_2) \in \mathbb{R}^2 \,|\, y_1 \geq 0, y_2 \leq 0\} \quad \textit{or matrix } \mathbf{W} := \begin{pmatrix} 1 & 0 \\ 0 & -1 \end{pmatrix} \textit{ in } (4.2)$$

imposing an alternative ordering structure in the objective space. The choice of $\mathbb{R}^2_{\geq 0}$ *as ordering cone is based on the intention not to prefer any of the two objectives to the other.*

- *The numerical evaluation of* $m_{\mathrm{d}}(\mathbf{T})$ *has been carried out using adaptive quadrature formulae with crude error tolerances of* 10^{-8}*. For the active-set methods in Step 4), we used error tolerances for* f_{obj} *and* $y = (\alpha_f, \alpha_m, \beta)^\top$ *of* $tol_{f,y} = 10^{-7}$*. The constraints were ensured for all iteration steps to be fulfilled to a tolerance of* $tol_{\mathrm{constr}} = 10^{-12}$*.*
- *Based on the range of results for Gen(*ϱ_∞*,* ϕ_0*), we performed a linear transformation (shift and scaling of* $m_{\mathrm{os}}(\mathbf{T})$ *and* $m_{\mathrm{d}}(\mathbf{T})$*) such that all resulting parameters have objective values in the positive orthant of* $\mathbb{R}^2$ *and are bounded by five. That way, it is secured that by using the nonlinear scalarizing functional* $z^{C,k}$ *all solutions of the vector optimization problem can be found and that we obtain a satisfactory distribution of points along the critical line if the vectors* k *are also equally distributed in* $\operatorname{int} C$*.*
- *From the construction principles stated above, we are initially faced with four types of constraints:*

  (a) The spectral radius of $\mathbf{T}$ *in the limit of infinite stiffness* $z \to \infty$ *has to be* equal *to* ϱ_∞ *as only then a fair comparison of the methods is possible. (That means that the absolute value of each eigenvalue has to be* smaller than or equal to ϱ_∞ *and, for at least one of the eigenvalues, equality is required.)*

  (b) The stability requirements of Proposition 2.1. need to be fulfilled. This imposes three linear *inequality constraints as zero stability is implied by unconditional stability for second order methods.*

  (c) The parameters of the method should be of moderate size such that the optimization algorithms do not approach theoretically relevant solution that, however, cannot be used in an actual implementation. We used the bounds

$$l_b \leq \alpha_f,\, \alpha_m,\, \beta \leq u_b\,, \qquad \text{with } l_b := -10\,,\ u_b := 10\,.$$

  (d) The second order condition (2.3) *was analytically eliminated, i. e., we used matrices* $\mathbf{T}(z)$ *in* (3.8) *and* $\mathbf{T}(\infty)$ *in* (3.9) *which already do not include the parameter* γ *anymore.*

Summarizing, this leads to a penalty function ϕ_{penalty} *of the following form:*

$$\begin{aligned}\phi_{\mathrm{penalty}}(\alpha_m, \alpha_f, \beta, \gamma) := {} & \frac{1}{\epsilon_{(\mathrm{a})}} \cdot \|\sigma(\mathbf{T}(\infty)) - \varrho_\infty\|_2 \\ & + \frac{1}{\epsilon_{(\mathrm{b})}} \left\| \min\left(\boldsymbol{b}_{(\mathrm{b})} - \mathbf{A}_{(\mathrm{b})} \begin{pmatrix} \alpha_f \\ \alpha_m \\ \beta \end{pmatrix}, \begin{pmatrix} 0 \\ 0 \\ 0 \end{pmatrix} \right) \right\|_2 \\ & + \frac{1}{\epsilon_{(\mathrm{c})}} \left(\left\| \min\left(\begin{pmatrix} u_b - \alpha_f \\ u_b - \alpha_m \\ u_b - \beta \end{pmatrix}, \begin{pmatrix} 0 \\ 0 \\ 0 \end{pmatrix} \right) \right\|_2 + \left\| \min\left(\begin{pmatrix} \alpha_f - l_b \\ \alpha_m - l_b \\ \beta - l_b \end{pmatrix}, \begin{pmatrix} 0 \\ 0 \\ 0 \end{pmatrix} \right) \right\|_2 \right),\end{aligned}$$

with penalty parameters $\epsilon_* \geq 0$ *for* $* \in \{(\mathrm{a}), (\mathrm{b}), (\mathrm{c})\}$ *and*

$$\mathbf{A}_{(\mathrm{b})} := \begin{pmatrix} -1 & 1 & 0 \\ \frac{1}{2} & -\frac{1}{2} & -1 \\ 1 & 0 & 0 \end{pmatrix}, \quad \boldsymbol{b}_{(\mathrm{b})} := \begin{pmatrix} 0 \\ \frac{1}{4} \\ \frac{1}{2} \end{pmatrix}.$$

The minimum in the penalization of inequality constraints is to be taken component-wise. Note that we did not square the norm since differentiability is no requirement for the Nelder-Mead algorithm. (Numerical tests using squared norms also gave inferior results.) For the results presented below we used rather strong penalization by setting

$$\epsilon_{(\mathrm{a})} = 10^{-10}\,, \quad \epsilon_{(\mathrm{b})} = 10^{-6}\,, \quad \epsilon_{(\mathrm{c})} = 10^{-1}\,,$$

taking into account that the equality constraint has to be almost exactly fulfilled to ensure comparability while a projection onto the piecewise linearly bounded convex set $\{y \in \mathbb{R}^3 \,|\mathbf{A}^{(b)} \cdot y \leq \boldsymbol{b}\}$ *is very easily done and the box constraints were taken rather arbitrarily anyway, see Remark 4.5.*

- *We used Matlab*^{TM},[1] *to carry out the optimization steps 1), 2), 3), and 4) and the preselection by Graef-Younes method in Step 5). Ensuring the constraint fulfillment to machine precision requires high precision computing which was done using Mathematica*®,[2].

In Figure 4 we display the numerical results for the very common setting $\varrho_\infty = 0.9$ which is known to cause relatively large overshoot for the Chung/Hulbert parameter choice but also popular for practitioners because of the good structure preservation. In the upper plot the results are displayed as they appear in the objective space $(m_{\mathrm{os}}^2(\mathbf{T}), m_{\mathrm{d}}(\mathbf{T}))$. It can be observed that the parameter choice of Chung/Hulbert [6] (magenta) is indeed the 'best' choice one can aim at when designing methods only with regards to an optimal dissipation behavior. The green and cyan markers/lines show the results for the well-established methods of Hilber/Hughes/Taylor and Wood/Bossak/Zienkiewicz, respectively. These methods are often favored to the parameter set of Chung/Hulbert because of their much lower overshoot tendency. The results show that the new parameter set from Section 3. can indeed be viewed as a compromise between the aforementioned candidates as the parameters smoothly transition away from the Chung/Hulbert point.
More importantly, it is revealed that neither the new parameter set $\mathrm{Gen}(\varrho_\infty,\ \phi_0)$ nor the well-established parameters of Hilber/Hughes/Taylor and Wood/Bossak/Zienkiewicz are efficient in the sense of Pareto optimality in the space overshoot-measure vs. dissipation measure. The highlighted methods will be used in the numerical experiments in Section 5. below and referenced by their enumeration in the plot.

$\varrho_\infty = 0.9$	α_m	α_f	β	γ
①	-9.268154485718	-9.000000000456	1.395330688022	0.768154485261
②	0.278333634277	0.340749149711	0.328502712812	0.562415515434
③	0.375191048106	0.429550535614	0.286102565819	0.554359487508
④	0.398295719396	0.451534067142	0.280201830242	0.553238347746

All requirements in the design paradigms above are fulfilled for the new parameter sets (except that we cannot just plug in the parameter ϱ_∞ but have to find the parameter values in a numerical way.) Also the additional requirement (e_2) (arrival at the trapezoidal rule for $\varrho_\infty \to 1$) cannot be guaranteed by the construction of the method but both requirements are only relevant for algorithms with explicit parameters, anyway.
Note that the objective function $(m_{\mathrm{os}}^2(\mathbf{T}), -m_{\mathrm{d}}(\mathbf{T}))$ is not convex; a simple linear scalarization would not have been able to find all the displayed solutions. The lower two plots in Figure 4 show a comparative view of the overall dissipation and overshoot behavior of all the displayed points in the objective space. It can be observed that the maximum overshoot as in the definition of $m_{\mathrm{os}}(\mathbf{T})$ may indeed be higher but on average the norm powers of $\mathbf{T}(\infty)$ decrease much faster for the new parameter sets than for the classical choices HHT and WBZ. From this, it can be expected (and we will indeed confirm this hypothesis numerically in Section 5. below) that the practically observed overshoot may in fact even be drastically less for $\mathrm{Gen}(\varrho_\infty,\phi_0)$ and the optimized methods.

5. NUMERICAL TESTS

In this section we will provide some insight on the actual performance gains that can be reached using the novel parameters developed so far. The implementation of the Newmark-type integrator is based on the pseudocodes given in [1], see also [12]. We restrict our experiments to constant time step sizes.

[1] MATLAB is a trademark of The MathWorks, Inc., `http://www.mathworks.com`
[2] MATHEMATICA is a registered trademark of Wolfram Research, Inc., `http://www.wolfram.com`

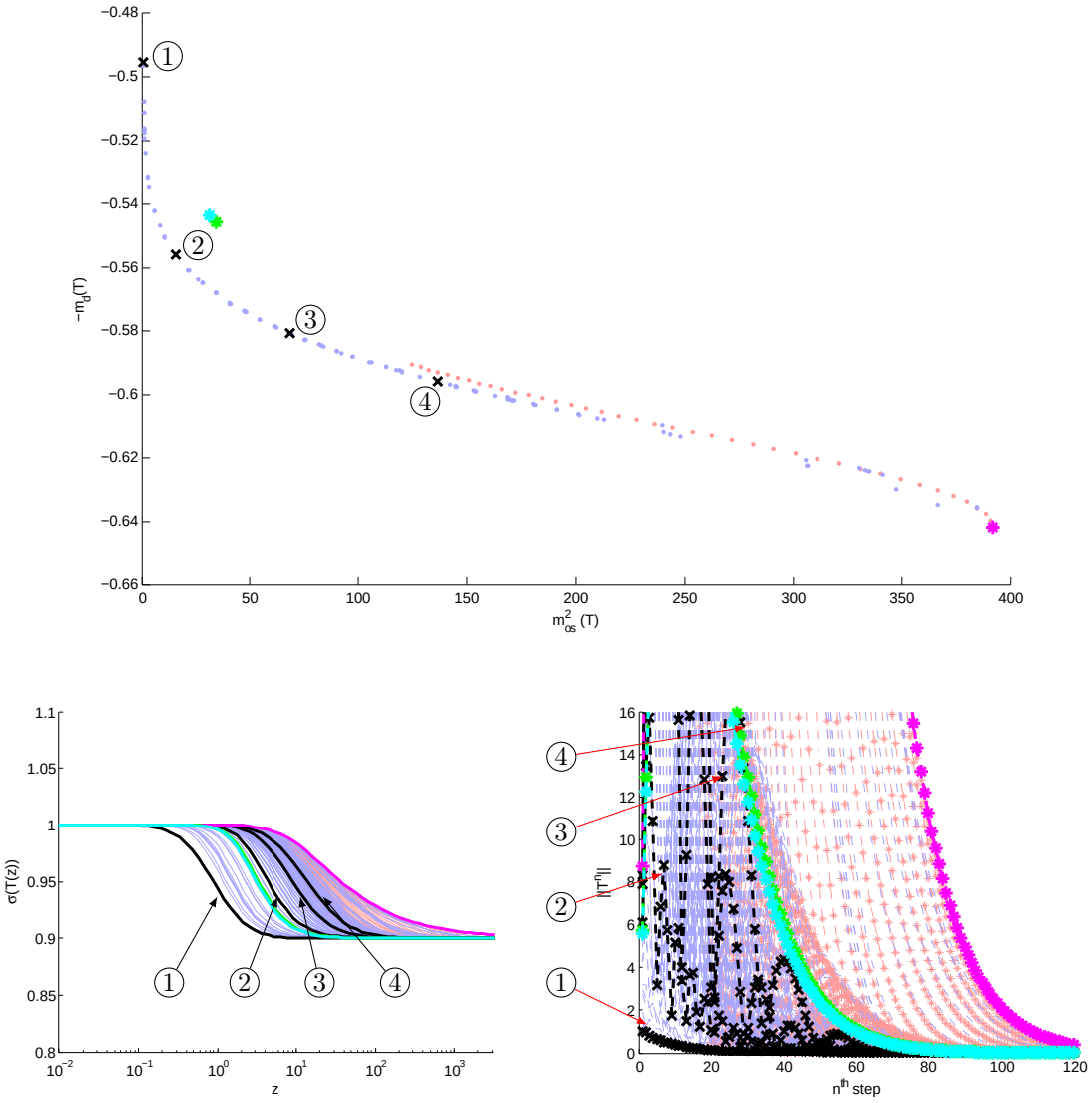

Figure 4: Top: New and old parameter sets in the objective space (m_{os}^2, m_{d}), Bottom left: Resulting dissipation behavior, Bottom right: Expected overshoot from 2-norm of matrix powers $\mathbf{T}^n$, In all plots: magenta: CH(0.9), green: HHT, cyan: WBZ, light red: Gen(0.9, ϕ_0) for $\phi_0 \in (0, \pi)$, light blue: Optimized methods, black: Four chosen representatives

For variable step size schemes there are various approaches known from the literature and we want to keep this presentation concise. The acceleration-like variable $\boldsymbol{a}_0$ is always initialized as this was originally proposed by in [6], i. e., $\boldsymbol{a}_0 := \ddot{\boldsymbol{q}}(t_0)$.
In Figure 5, we display the numerical solution (some chosen components of the Lagrange multiplier $\boldsymbol{\lambda}(t)$) for the well-known benchmark "Andrews Squeezer Mechanism", see [16, 27]. The problem is formulated in Carthesian coordinates of the centers of mass of the seven bodies in the plane leading to a differential-algebraic system of dimension $n_{\boldsymbol{q}} + n_{\boldsymbol{\lambda}} = 41$. The dynamic equations are described and solved in their index-3 formulation; from the literature [5], it is known that this description is particularly prone to overshoot. We used a numerical damping of $\varrho_\infty = 0.95$ and a time step size of $h = 10^{-5}$. The initial values where computed from a very accurate numerical solution of the initial values given in [16] at $t_0 = 0.01$ which where then additionally projected to the constrained manifold on position and velocity level such that they are consistent to machine precision. We did not use the original initial values for this benchmark since it is known [2] that for vanishing initial velocities, algorithm (2.2) does not show overshoot.
It can be observed that for all three experiments overshoot is apparent, yet the algorithm of Hilber, Hughes, and Taylor (HHT), see (3.2), shows considerably less overshoot than the parameter settings of Chung and Hulbert (CH), see (3.1). The new parameters from (3.12) perform even better and the numerical results are in good agreement to the more theoretical predicted error amplifications from Figure 3.

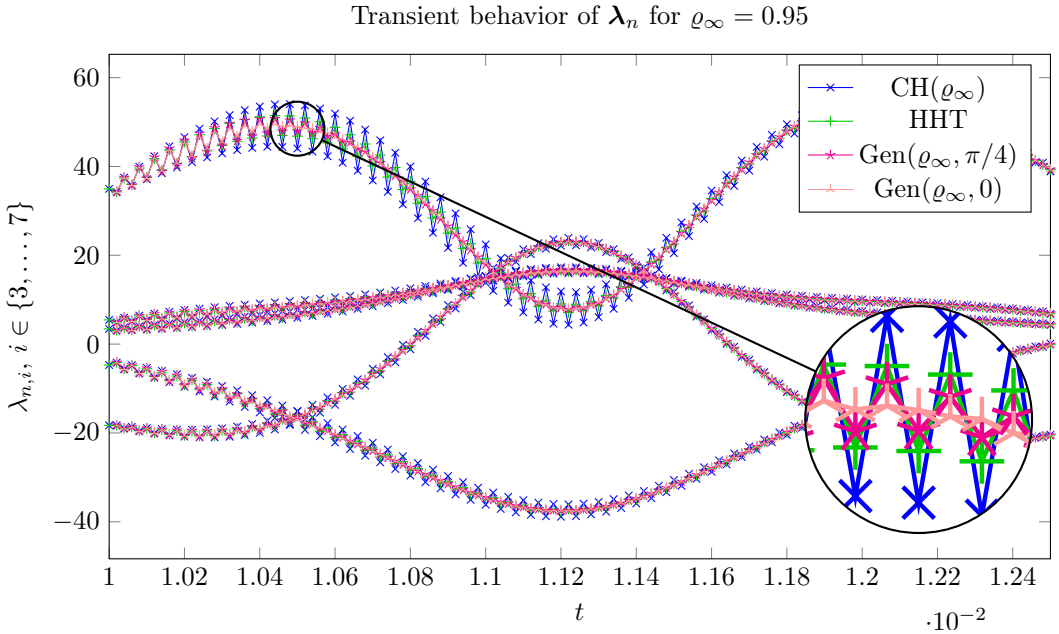

Figure 5: Observed overshoot in the numerical approximations of selected Lagrange multipliers for CH(ϱ_∞), HHT, and the new parameter set Gen(ϱ_∞, ϕ_0) for the benchmark "Andrews Squeezer Mechanism"

The second test benchmark was developed in [28] and describes the planar motion of a crank mechanism with a flexible crank shaft that is propelled to have a constant angular velocity. The flexible crank's deformation is approximated using a finite-element approach with polynomial Galerkin functions for the longitudinal and sine functions for vertical displacements with a nonlinear model describing the internal strain energy. It is particularly suited as a test benchmark since

(i) it includes external input forces (known to cause higher overshoot),

(ii) its construction as a lumped parameter surrogate model makes it an ideal benchmark for applications with coupled PDE-DAE problems,

(iii) as the 'squeezer mechanism' example above, it is one of the best studied benchmarks in the multibody system community.

The system has $n_{\boldsymbol{q}} = 7$ differential variables constrained by $n_{\boldsymbol{\lambda}} = 3$ algebraic conditions and allowing for four degrees-of-freedom. In Figure 6 we show the numerical approximations of the three

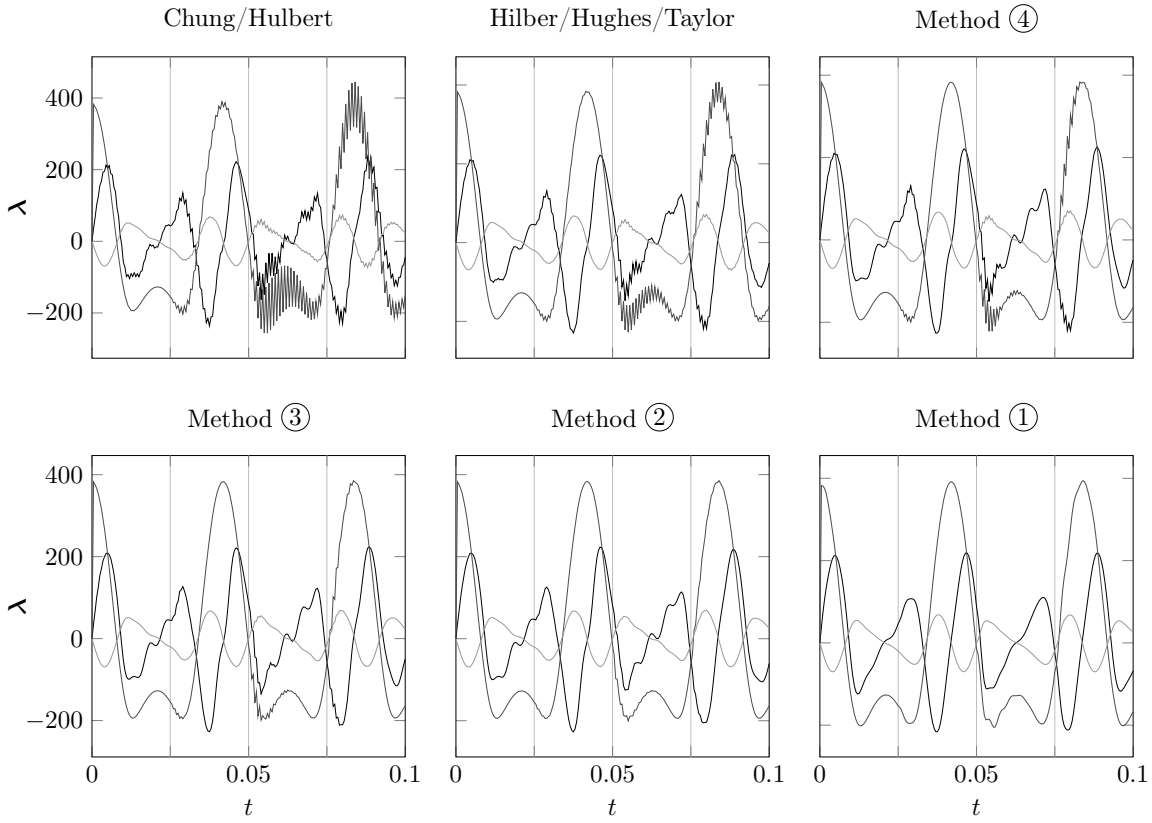

Figure 6: Numerical results (approximation of Lagrange multipliers) for the slider crank benchmark using classical and optimized Newmark-type methods

Lagrange multipliers. In all experiments, we used $h = 5 \cdot 10^{-4}$ and projected the velocity coordinates after $n_{\text{proj}} = 50$ time integration steps to fulfill the constraints on velocity level, i.e., adapted the numerical approximations $\boldsymbol{v}_n$ such that not only $\boldsymbol{\Phi}(t_n, \boldsymbol{q}_n, \boldsymbol{v}_n, \boldsymbol{\lambda}_n) = \boldsymbol{0}$ is fulfilled but also $(\mathrm{d}\boldsymbol{\Phi})/(\mathrm{d}t)|_{(t,\boldsymbol{q},\boldsymbol{v},\boldsymbol{\lambda})=(t_n,\boldsymbol{q}_n,\boldsymbol{v}_n,\boldsymbol{\lambda}_n)} = \boldsymbol{0}$. The time instances where projection is applied are marked in Figure 6 by gray vertical lines. It has been reported in the literature [3] that velocity projection can cause Newmark-type integrators to show overshoot behavior even beyond the transient phase of the time integration.
Indeed, one can observe that for the CH, the HHT, and method ④ (first row) rather heavy overshoot occurs, while the numerical solutions for the other three methods (second row) remain smooth. In each step, the nonlinear systems are solved using the Newton-Raphson method with a first order

approximation of the Jacobi matrix. The computational advantage of the smoother approximation can also be measured with regards to the average number of Newton-Raphson iterations (which for large scale problems often states the most computational effort). In our experiments it drops from 4.8358 for CH(0.9) over 4.4726 and 4.2736 for HHT and method ④, respectively, to 4.1393 and 4.0945 for methods ③ and ②. For method ① this decrease is no longer present but instead the average number increases again to 4.5522. This can be explained by the inferior accuracy for this method implied by a large third order error constant.

6. CONCLUSION AND ASPECTS OF FURTHER RESEARCH

Using the theoretical background of the one-step error analysis of Newmark-type integrators we derived a novel parameter set Gen(ϱ_∞,ϕ_0). In particular, the degenerate Jordan canonical form for the test equation of the harmonic oscillator in the limit of infinite frequency can be seen as one of the main reasons for spurious and unphysical oscillations in the numerical approximation. So, the basic idea behind the new method is to choose the parameters in a way that this behavior is decimated. Numerical results show an improvement with respect to overshoot.

Furthermore, we presented a mathematical framework that allowed for a systematic optimization of this important class of time integration methods in technical simulations with respect to two of the main requisites from a practical/experimental viewpoint. On the one hand, the dissipation behavior over the entire frequency-range was taken into account, but on the other hand we also included the overshoot-problem into the method's design which has not been done for the established parameter sets of Chung/Hulbert, Hilber/Hughes/Taylor and Wood/Bossak/Zienkiewicz. Well-established nonlinear scalarization methods from vector optimization were substantial for gaining an encompassing understanding of the analytical properties of the integration family. Small numerical examples show that this approach can in fact have a tremendous impact on the quality of the numerical approximation.

For the proposed class of algorithms, there are other ways (see for example [2]) to overcome overshoot analytically by adapting the initial values on velocity level in a way to avoid error artifacts that are later on amplified from the very start. This approach, however, requires additional knowledge of certain values in the model that might not be so easily computed (and depend on a certain problem structure) and involves changes in the implementation, while our concept can be used to adapt existing codes right away.

In a more general setting and depending on the application cases at hand, one might—as a next step—take more aspects of the algorithm's design into account and treat them as additional objectives. Other possible measures include, for example, dispersion, relative period error [21] and the error constants of the third order error terms in the Taylor expansion [16]. It is also possible to tailor the optimization for other special application cases like strongly damped mechanical systems [29]. This would indeed require some extensions of the involved terms, as in that case we need to consider (3.5) with $\xi > 0$.

Some authors recommend that the spurious root should remain zero when $z \to 0$ in (3.7) (a property called "optimal zero-stability"). This would pose an additional constraint in the optimization problem. The technical necessities for an extension to this more general analysis are all available in the framework presented in Section 4.

Here, we did not explore the scalarization functional fully. For specific applications one might be interested in weighting certain areas in the objective space which could be accomplished by the use of different ordering cones or even variable ordering. The approach taken here is very general and can therefore be generalized to this case in a straightforward way.

In the numerical experiments, we saw that the new parameter sets outperform the classical algorithms much better than would be expected from the simple comparison of the values of the measure of overshoot as given in Definition 4.1. above. That is evident from the fact that, practically speaking, overshoot is not only to be measured by magnitude but also by its duration. So, alternatively, one could also think of a discrete measure like 'overshoot is the exponent of the first matrix power with a lower norm than $\mathbf{T}$ itself' or take an integral value for the definition of overshoot. For some applications, a

steeper decline of spectral radius might be considered superior to a gradual descent since this stronger resembles the frequency behavior of an optimal low-pass filter.
At last, one could also consider an extension to the more general class of algorithms like the one that was proposed in [19, 20] and includes algorithm (2.2) as a special case. These more intricate algorithms might require to interpret the search for optimal damping measure as an optimal control problem or base the analysis on the amplification matrices pseudospectra [31] whose study might provide an even better understanding.

RECEIVED: SEPTEMBER, 2017.
REVISED: JANUARY, 2018.

REFERENCES

[1] ARNOLD, M. AND BRÜLS, O. (2007): Convergence of the generalized-α scheme for constrained mechanical systems **Multibody Syst. Dyn.**, 18:185–202.

[2] ARNOLD, M., BRÜLS, O., AND CARDONA, A. (2015a): Error analysis of generalized-α Lie group time integration methods for constrained mechanical systems **Numer. Math.**, 129:149–179.

[3] ARNOLD, M., BRÜLS, O., AND CARDONA, A. (2015b): Order reduction in time integration caused by velocity projection **J. Mech. Sci. Tech.**, 29(7):2579–2585 revised and extended version published as Technical Report 02-2015, Martin Luther University Halle-Wittenberg, Institute of Mathematics.

[4] ARNOLD, M., CARDONA, A., AND BRÜLS, O. (2016): A Lie algebra approach to Lie group time integration of constrained systems In Betsch, P., editor, **Structure-Preserving Integrators in Nonlinear Structural Dynamics and Flexible Multibody Dynamics**, volume 565 of **CISM Courses and Lectures**, pages 91–158. Springer International Publishing Preliminary version, published as Technical Report 01-2015, Martin Luther University Halle-Wittenberg, Institute of Mathematics.

[5] CARDONA, A. AND GÉRADIN, M. (1989): Time integration of the equations of motion in mechanism analysis **Compututers & Structures**, 33(3):801–820.

[6] CHUNG, J. AND HULBERT, G. (1993): A time integration algorithm for structural dynamics with improved numerical dissipation: the generalized-α-method **J. Appl. Mech.**, 60:371–375.

[7] CONSOLE, P. AND HAIRER, E. (2014): Long-term stability of symmetric partitioned linear multistep methods In Dieci, L. and Guglielmi, N., editors, **Current Challenges in Stability Issues for Numerical Differential Equations**, volume 2082 of **Lecture Notes in Mathematics**, pages 1–37. Springer International Publishing.

[8] DAHLQUIST, G. (1963): A special stability problem for linear multistep methods **BIT Numer. Math.**, 3(1):27–43.

[9] DAHLQUIST, G. (1978): On accuracy and unconditional stability of linear multistep methods for second order differential equations **BIT Numer. Math.**, 18(2):133–136.

[10] EICH-SOELLNER, E. AND FÜHRER, C. (1998): **Numerical Methods in Multibody Dynamics** B. G. Teubner Stuttgart.

[11] ERLICHER, S., BONAVENTURA, L., AND BURSI, O. (2002): The analysis of the generalized-α method for non-linear dynamic problems **Comput. Mech.**, 28:83–104.

[12] GÉRADIN, M. AND RIXEN, D. (2015): **Mechanical vibrations – Theory and application to structural dynamics** John Wiley & Sons, Ltd., 3rd edition.

[13] GERTH (TAMMER), C. AND WEIDNER, P. (1990): Nonconvex separation theorems and some applications in vector optimization **J. Optim. Theory Appl.**, 67(2):297–320.

[14] GÖPFERT, A., RIAHI, H., TAMMER, C., AND ZĂLINESCU, C. (2003): **Variational Methods in Partially Ordered Spaces** CMS Books in Mathematics. Springer-Verlag, New York.

[15] HAIRER, E., LUBICH, C., AND WANNER, G. (2006): **Geometric Numerical Integration** Number 31 in Springer Series in Computational Mathematics. Springer, Berlin Heidelberg, 2nd edition.

[16] HAIRER, E. AND WANNER, G. (2002): **Solving ordinary differential equations part II - Stiff and differential-algebraic problems** Number 14 in Springer Series in Computational Mathematics. Springer Berlin Heidelberg, 2nd edition.

[17] HILBER., H. AND HUGHES, T. (1978): Collocation, dissipation and 'overshoot' for time integration schemes in structural dynamics **Earthq. Eng. Struct. Dyn.**, 6:99–117.

[18] HILBER, H., T. HUGHES, AND TAYLOR, R. (1977): Improved numerical dissipation for time integration algorithms in structural dynamics **Earthq. Eng. Struct. D.**, 5:99–118.

[19] HOFF, C. AND PAHL, P. (1988a): Development of an implicit method with numerical dissipation from a generalized single-step algorithm for structural dynamics **Comput. Meth. Appl. Mech. Engrg.**, 67:367–385.

[20] HOFF, C. AND PAHL, P. (1988b): Practical performance of the θ_1 method and comparison with other dissipative algorithms in structural dynamics **Comput. Meth. Appl. Mech. Engrg.**, 67:87–110.

[21] HUGHES, T. (1987): **The finite element method: Linear static and dynamic finite element analysis** Prentice-Hall, Inc. Englewood Cliffs, NJ.

[22] JAHN, J. (2011): **Vector Optimization** Springer-Verlag, Berlin Heidelberg, 2nd edition.

[23] KÖBIS, M. (2016): **A family of Newmark-type methods for singularly perturbed mechanical systems** PhD thesis, Martin Luther University Halle–Wittenberg.

[24] NELDER, J. AND MEAD, R. (1965): A simplex method for function minimization **Computer Journal**, 7(4):308–313.

[25] NEWMARK, M. (1959): A method of computation for structural dynamics **J. Eng. Mech. Div.**, 85(EM 3):67–94 Proc. of ASCE.

[26] NOCEDAL, J. AND WRIGHT, S. (1999): **Numerical Optimization** Springer Series in Operations Research. Springer-Verlag New York.

[27] SCHIEHLEN, W. (1990): **Multibody system handbook** Springer New York Heidelberg.

[28] SIMEON, B. (1996): Modelling a flexible slider crank mechanism by a mixed system of DAEs and PDEs **Math. Model. Sys.**, 2(1):1–18.

[29] STUMPP, T. (2008): Asymptotic expansions and attractive invariant manifolds of strongly damped mechanical systems **Z. Angew. Math. Mech.**, 88:630–643.

[30] TAMMER, C. AND WINKLER, K. (2003): A new scalarization approach and applications in multicriteria d.c. optimization **J. Nonlinear Convex Anal.**, 4(3):365–380.

[31] TREFETHEN, L. AND EMBREE, M. (2005): **Spectra and Pseudospectra: The Behavior of Nonnormal Matrices and Operators** Princeton University Press.

[32] WOOD, W., BOSSAK, M., AND ZIENKIEWICZ, O. (1981): An alpha modification of Newmark's method **Int. J. Numer. Meth. Eng.**, 5:1562–1566.

[33] YOUNES, Y. (1993): **Studies on dicrete vector optimization** PhD thesis, University of Demiatta (Egypt).

A STABILITY NOTIONS IN MULTIBODY SYSTEM DYNAMICS

Definition A1. (Stability Concepts) *Consider the integration method* (2.2) *applied to the linear test equation* (3.5)*. We say that the method is*

1. zero-stable *if there exists an* $h_0 > 0$ *such that in exact arithmetics the method provides bounded solutions on finite time horizons* $t \in [t_0, t_{\text{end}}]$ *for* $\omega = \xi = 0$ *and any* $h < h_0$*,*
2. *optimally zero-stable if it is zero stable and, additionally, the amplification matrix* $\mathbf{T}(0)$ *has one eigenvalue that is exactly zero,*
3. (linearly) stable at infinity *if the amplification matrix* $\mathbf{T}(\infty)$ *has a spectral radius less or equal to one,*
4. strictly (linearly) stable at infinity *if the amplification matrix* $\mathbf{T}(\infty)$ *has a spectral radius strictly less than one,*
5. unconditionally (linearly) stable *(or I-stable) if for all* $\omega \in [0, \infty)$ *the spectral radius of* $\mathbf{T}(z)$ *for* $z := h\omega$ *is bounded by one, (In particular, this includes stability at infinity.)*
6. L-stable *if it unconditionally stable and additionally all eigenvalues of* $\mathbf{T}(\infty)$ *vanish,*
7. internally stable *if it is zero-stable and the requirement of using exact arithmetics in the definition of zero-stability can be dropped.*

If the method is zero-stable, unconditionally stable and strictly stable at infinity, we just refer to it as stable*. Note that in the literature, the term 'stable' is often used equivalently to zero-stability.*